*Detailed Response to Reviewers

Professor Dag Myrhaug
Department of Marine Technology
Norwegian University of Science and Technology
NO-7491 Trondheim, Norway
Email: dag.myrhaug@ntnu.no

30th April, 2015

Editors
Ocean Engineering

Manuscript No.:OE-D-14-00197
Title: "SUSPENDED SEDIMENTS DUE TO RANDOM WAVES INCLUDING EFFECTS OF SECOND ORDER WAVE ASYMMETRY AND BOUNDARY LAYER STREAMING"
Authors: Dag Myrhaug, Muk Chen Ong and Lars Erik Holmedal

Dear Editors,

Please find enclosed the revised manuscript referred to, submitted for possible publication in Ocean Engineering.
The reviewer's comments have been addressed as follows:

Reviewer #1:
Major modifications:

1. The reference given deals with sheet flow for steady flow and is therefore not relevant to compare with. Moreover, as stated in the first paragraph of Section 4, no data exist (to the authors' knowledge) in the open literature on suspended concentration for random wave-induced sheet flow; therefore an example of results is provided.
2. The predictions can probably be improved by "tuning" the reference concentration to the four data sets. However, due to the limited data available to compare with this is not made here, but could be an issue when more data for random wave conditions become available.
3. This issue is already considered to be addressed in the second last paragraph of Section 4.1.
4. We agree with the reviewer's comment; this suggests the need for more experimental data for validation.

Minor modifications:

1. to 8.; all these issues have been taken into account and modifications are included in the revised manuscript.

Yours sincerely,

Dag Myrhaug

SUSPENDED SEDIMENTS DUE TO RANDOM WAVES INCLUDING EFFECTS OF SECOND ORDER WAVE ASYMMETRY AND BOUNDARY LAYER STREAMING

by

Dag Myrhaug[1], Muk Chen Ong[2] and Lars Erik Holmedal[1]
[1]Department of Marine Technology
Norwegian University of Science and Technology
NO-7491 Trondheim, NORWAY
[2]Norwegian Marine Technology Research Institute (MARINTEK)
NO-7450 Trondheim, Norway
E-mail: dag.myrhaug@ntnu.no
Phone: +4773595527

Abstract: The paper provides a practical stochastic method by which the suspended sediment concentration due to long-crested (2D) and short-crested (3D) nonlinear random waves can be calculated. The approach is based on assuming the waves to be a stationary narrow-band random process, and by using the parameterized formulas valid for regular waves presented in Soulsby (1997). The Forristall (2000) wave crest height distribution representing both 2D and 3D nonlinear random waves is also adopted. The model covers sediment suspension over rippled beds and for sheet flow. Comparisons are made with random wave data from Thorne et al. (2002) for flow over rippled beds. An example for sheet flow using data typical to field conditions is also included to illustrate the approach.

Keywords: *Suspended sediment concentration, Rippled bed, Sheet flow, Second order wave asymmetry, Wave boundary layer streaming, Nonlinear random waves, Stochastic method.*

1. INTRODUCTION

Suspended sediment concentrations over sandy seabeds in shallow and intermediate water depths, i.e. in coastal zones and on continental shelves, occur predominantly as a result of the combined action of waves and currents. The waves are the principal cause of the entrainment of the sediment, which are diffused into the flow by turbulent processes, and subsequently transported by the current. Wave-current-sediment interactions are crucial in scour and erosion studies for seabed pipelines and other near seabed structures. This interaction is also important in developing models for the movement of sediment on the seabed in combined action of waves and currents, and the resulting coastal evolution.

In a realistic sea state the surface waves show a complex three-dimensional irregular pattern where the sharpening of the wave crests manifests wave nonlinearity, complicating the problem. The wave-induced bottom shear stress determines the response of sandy seabeds. When the shear stress exceeds the critical value for initiation of sand motion, ripples will be formed as the wave activity increases. Under large waves the seabed ripples are washed out such that a larger layer of high sediment concentration is developed in the vicinity of the bed, i.e. a sheet flow layer with a thickness of the order of mm or cm depending on how it is defined (see e.g. Myrhaug and Holmedal (2007)).

The sheet flow layer is defined as the layer where concentrations are so high that inter-granular forces and sediment flow interaction forces are important. Sheet flow transport is important in the surf zone even in moderate wave conditions, and the associated high concentrations play an important role in erosion, sedimentation and morphology as well as for the design of coastal structures. Under severe wave conditions sheet flow may occur in intermediate water depths, and the intense sediment transport might cause exposure of e.g. buried pipelines and foundations of structures, as well as affect the stability of scour protections of marine structures. Sheet flow conditions might also have ecological

implications since the high sand concentrations might directly affect life in the ocean in several ways: for example, highly turbid water might negatively impact fish to feed, as well as reducing their reproduction rate. Thus, knowledge of the response of this thin layer for sheet flow under realistic field conditions is crucial to conserve the diversity of species living in the thin surface bottom sediment layer. The suspended sediments also play an important role in spreading and transport of pollutants, since it affects the upper bottom sediment layer which is brought into suspension. Recent works related to sheet flow are those of e.g. Myrhaug and Holmedal (2007); Holmedal et al. (2013); Fuhrman et al. (2013); Chassagneux and Hurther (2014); and the references therein.

Steady streaming under sinusoidal waves is caused by non-uniformity of the wave boundary layer resulting from spatial variation of the orbital velocities. Vertical velocities generated within the bottom boundary layer under progressive waves are not exactly out of phase with the horizontal velocities, leading to a non-zero time-averaged bed shear stress. The steady streaming for a laminar wave boundary layer was determined by Longuet-Higgins (1956). Based on this work, the streaming-related time-averaged bed shear stress can be expressed in terms of the wave friction factor and the wave number (see, e.g. Nielsen (1992)). Nielsen and Callaghan (2003) included the effect of streaming predicting the shear stress and the total sediment transport rate for sheet flow under waves. The effect of streaming was included by adding a constant shear stress corresponding to the streaming-related bed shear stress and by applying a friction factor for rough turbulent flow. This method predicts the real propagating wave observations of Ribberink et al. (2000) quite well. Myrhaug et al. (2004) followed Nielsen and Callaghan (2003) relating the wave-induced current (streaming) for rough turbulent flow and used this to deduce formulas for bottom friction and bedload sediment transport due to boundary layer streaming beneath random waves. The effects of second order wave asymmetry on bottom friction and bedload sediment transport for

horizontally uniform oscillatory flow were also part of the study.

A summary of results from models and experiments on wave-induced streaming near the seabed is given by Davies and Villaret (1997, 1998, 1999). Above a smooth bed, the measured streaming at the edge of the wave boundary layer is in reasonable agreement with the Eulerian drift predicted by Longuet-Higgins (1956). Over a flat rough bed, however, the Eulerian drift is reduced in magnitude. The reason is that the phase difference between the outer velocity and the near-bed velocity is smaller for rough turbulent flow than for laminar flow. This feature is described by Trowbridge and Madsen (1984) for flows in which momentum transfer is dominated by turbulent processes, i.e. for $A/z_0 \geq 900$, where A is the near-bed orbital displacement amplitude and z_0 is the bed roughness. Trowbridge and Madsen (1984) also included the effect of second order wave asymmetry by including second order terms in a specified time-varying eddy viscosity for flow over flat rough beds. They found that this reduced the Eulerian drift at the edge of the boundary layer with a mean flow reversal (negative drift) occurring for very long waves, i.e. for small kh, where k is the wave number and h is the water depth.

Holmedal and Myrhaug (2009) investigated in detail the Longuet-Higgins streaming, the streaming due to wave asymmetry and the interaction between these two mechanisms. For realistic physical situations the seabed boundary layer beneath both propagating linear waves and Stokes second order waves, as well as horizontally uniform oscillatory bottom boundary layer flow with second order asymmetric forcing were investigated. They found that the Longuet-Higgins streaming velocities beneath propagating linear waves are always in the wave propagation direction, while the streaming velocities in horizontally uniform boundary layers with asymmetric forcing are opposite the wave propagation direction. This work was extended by Holmedal et. al. (2013) investigating the effect of streaming on the seabed boundary layer flow beneath combined waves and current for waves following and opposing a

current. They found that for wave-dominated conditions the mean (i.e. averaged over one wave period) velocity profile beneath following waves and current is significantly different from the mean velocity profile beneath opposing waves and current. Both linear and second order Stokes waves were taken into account (a review and more details are given in Holmedal et. al. (2013) and in the references therein).

The reader should note the difference between the two effects considered in this work; the second order wave asymmetry and streaming. Due to the second order wave asymmetry effect, the magnitude of the wave crest velocity is larger than that of the wave trough velocity at the edge of the boundary layer. On the other hand, streaming is caused by the presence of a vertical velocity component in the boundary layer under progressive waves giving a weak current at the edge of the boundary layer. For the parameter regime considered here, this current is in the wave propagation direction.

For the prediction of suspended sediment concentration due to random waves, a commonly used procedure is to substitute the wave-related quantities with their characteristic statistical values, for example the *rms* (root-mean-square) values in an otherwise deterministic approach, see e.g. Soulsby (1997). Comparison of results from field measurements and empirical models of suspended sediments under waves and currents have been made by representing the random waves by their characteristic statistical values (see e.g. Cacchione et al. (2008), Dolphin and Vincent (2009), Bolanos et al. (2012)). However, this procedure does not account for the stochastic feature of the processes included. Moreover, sharpening of the wave crests manifests wave-nonlinearity. To the present authors knowledge no stochastic method for prediction of suspended sediment concentration beneath random waves is available in the open literature.

The purpose of this study is to provide a practical stochastic method for calculating the suspended sediment concentration over rippled seabeds and for sheet flow due to random

waves including effects of second-order wave asymmetry. For sheet flow the effect of wave boundary layer streaming is also provided. The approach is based on assuming the waves to be a stationary narrow-band random process, adopting the Forristall (2000) wave crest height distribution representing both long-crested (2D) and short-crested (3D) random waves, and using parameterized formulas valid for regular waves presented in Soulsby (1997). The model covers sediment suspension over rippled beds for linear and 2D nonlinear random waves, and comparisons are made with data obtained from measurements of suspended sediment concentrations over rippled bedforms beneath 2D random waves in a large-scale flume reported by Thorne et al. (2002). An example for sheet flow is also included to demonstrate the applicability of the results for practical purposes using data typical for field conditions.

2. SUSPENDED SEDIMENTS DUE TO REGULAR WAVES

Many parameterizations to calculate the suspended sediment concentration in the water column close to the seabed under regular waves have been proposed in the literature; these parameterizations were reviewed and presented in Soulsby (1997). In the following the formulas for regular waves, which are used as the basis for suspended sediments due to random waves given in Section 3, will be summarized.

2.1 Rippled beds

For rippled beds the concentration profile is given by

$$C(z) = C_0 \exp\left(-\frac{z}{\ell}\right) \tag{1}$$

where $C(z)$ is the sediment concentration at the height z above the bed, C_0 is the reference concentration at the seabed, and ℓ is the decay length scale. Here the Nielsen (1992) expressions for ℓ and C_0 are adopted

$$\ell = 0.075\frac{U}{w_s}\eta \quad \text{for} \quad \frac{U}{w_s} < 18 \tag{2}$$

$$\ell = 1.4\eta \quad \text{for} \quad \frac{U}{w_s} \geq 18 \tag{3}$$

$$C_0 = 0.005\theta_r^3 \quad ; \quad \theta_r = \frac{\theta}{\left(1-\pi\frac{\eta}{\lambda}\right)^2} \tag{4}$$

Here U is the linear near-bed orbital velocity amplitude, w_s is the settling velocity, η is the ripple height, λ is the ripple length, and θ is the Shields parameter defined by

$$\theta = \frac{\tau_w}{\rho g(s-1)d_{50}} \tag{5}$$

Here τ_w is the maximum bottom shear stress under the waves, ρ is the density of the fluid, g is the acceleration due to gravity, s is the sediment density to fluid density ratio, and d_{50} is the median diameter of grains.

The maximum bottom shear stress within a wave cycle is taken as

$$\frac{\tau_w}{\rho} = \frac{1}{2} f_w U^2 \tag{6}$$

where f_w is the friction factor, which is taken from Myrhaug et al. (2001, Table 3)

$$f_w = c\left(\frac{A}{z_0}\right)^{-d} \tag{7}$$

$$(c,d) = (18,1) \quad \text{for} \quad 20 \lesssim A/z_0 \lesssim 200 \tag{8}$$

$$(c,d) = (1.39,0.52) \quad \text{for} \quad 200 < A/z_0 \lesssim 11000 \tag{9}$$

$$(c,d) = (1.12,0.25) \quad \text{for} \quad 11000 < A/z_0 \tag{10}$$

where $z_0 = 2.5d_{50}/30$ is the bed roughness used in Eqs. (6) to (10) to calculate the shear stress due to the grain size, $A = U/\omega$ is the maximum near-bed orbital displacement, and ω is the wave frequency. Note that Eq. (9) corresponds to the coefficients given by Soulsby

(1997) obtained as best fit to data for $10 \lesssim A/z_0 \lesssim 10^5$.

The settling velocity is obtained from Soulsby (1997) as

$$w_s = \frac{\nu}{d_{50}}\left[\left(10.36^2 + 1.049 D_*^3\right)^{1/2} - 10.36\right] \tag{11}$$

where ν is the kinematic viscosity of the fluid and D_* is the dimensionless grain diameter defined as

$$D_* = \left[\frac{g(s-1)}{\nu^2}\right]^{1/3} d_{50} \tag{12}$$

For irregular wave-generated ripples the Nielsen (1992) expressions for η and λ are adopted:

$$\eta = 21\psi^{-1.85} A \quad \text{for } \psi > 10 \tag{13}$$

$$\frac{\eta}{\lambda} = 0.342 - 0.340\theta^{0.25} \tag{14}$$

where ψ is the mobility number defined by

$$\psi = \frac{U^2}{g(s-1)d_{50}} \tag{15}$$

The ripples are washed out for $\theta \geq 0.8$. According to Nielsen (1992) θ, ψ and A in Eqs. (13) and (14) are based on using the significant wave height H_s. However, in the present method H_{rms} will be used. More discussion will be given in Section 3.

It should be noted that ripples start to be generated when $\theta > \theta_{cr}$, where θ_{cr} is the critical value of the Shields parameter corresponding to the initiation of motion at the bed which according to Soulsby (1997) is given as

$$\theta_{cr} = \frac{0.30}{1+1.2D_*} + 0.05\left[1 - \exp(-0.020D_*)\right] \tag{16}$$

As already mentioned the wave ripples are washed out leaving a flat bed with oscillatory sheet flow, when the criterion is given in terms of $\theta \geq 0.8$.

2.2 Sheet flow

For sheet flow conditions the concentration profile is given by

$$C(z) = C_a \left(\frac{z}{z_a} \right)^{-b} \tag{17}$$

where the Zyserman and Fredsøe (1994) expressions for the reference height z_a and the reference concentration C_a are adopted; $z_a = 2.0 d_{50}$ and

$$C_a = \frac{0.331(\theta - 0.045)^{1.75}}{1 + 0.720(\theta - 0.045)^{1.75}} \tag{18}$$

Moreover, $b = w_s / (\kappa u_*)$, and is based on assuming the eddy diffusivity to vary linearly with the distance from the seabed, $\kappa = 0.4$ is von Karman's constant, $u_* = (\tau_w / \rho)^{1/2}$ is the friction velocity, which by using Eq. (5) can be expressed in terms of the Shields parameter as

$$u_* = \left[g(s-1) d_{50} \theta \right]^{1/2} \tag{19}$$

2.2.1 Effect of streaming

The effect of streaming is included by adopting the results in Myrhaug et al. (2004) (following Nielsen and Callaghan (2003)), taken as a linear combination of the bed shear stress for waves and streaming, which is not strictly true due to nonlinear interaction. However, as a first approximation the streaming is considered to give an additional shear stress, i.e. the Shields parameter can be written as

$$\theta_t = \theta + \theta_{str} \tag{20}$$

where θ_{str} is the Shields parameter associated with the boundary layer streaming given by

$$\theta_{str} = \frac{\tau_{str}}{\rho g(s-1) d_{50}} \; ; \; \tau_{str} = \frac{1}{4\sqrt{2}} k A f_w U^2 \tag{21}$$

It should be noted that the approach is valid for $A/z_0 \gtrsim 900$, i.e. by using Eqs. (7), (9) and (10) for $A/z_0 \gtrsim 900$. Further details are given in Myrhaug et al. (2004).

By combining Eqs. (5), (6), (20) and (21), Eq. (20) can be rearranged to

$$\theta_t = \theta(1+\delta) \; ; \; \delta = \frac{1}{2\sqrt{2}} kA \tag{22}$$

Thus, the effect of streaming on the concentration profile can be taken into account by using Eqs. (11), (12), (17) to (19) with θ_t replacing θ, i.e. Eqs. (18) and (19) are replaced by, respectively:

$$C_a = \frac{0.331\left[\theta(1+\delta)-0.045\right]^{1.75}}{1+0.720\left[\theta(1+\delta)-0.045\right]^{1.75}} \tag{23}$$

$$u_* = \left[g(s-1)d_{50}\theta(1+\delta)\right]^{1/2} \tag{24}$$

3. SUSPENDED SEDIMENTS DUE TO NONLINEAR RANDOM WAVES

3.1 Theoretical background for stochastic method

Under nonlinear waves the nonlinearity is primarily caused by the asymmetric wave velocity, i.e. that the near-bed orbital velocity is larger in the wave propagation direction than in the opposite direction. In the present paper the effects of wave asymmetry are considered by using Stokes second-order wave theory. For Stokes second-order waves the nonlinearity is primarily caused by the larger velocity under the wave crest (crest velocity) than under the wave trough (trough velocity). It seems reasonable that it is the largest velocity in the wave cycle (i.e. the crest velocity) which is responsible for bringing sand grains into suspension, rather than the mean of the crest and the trough velocity (i.e. equal to the linear wave velocity). Thus the concentration for individual random Stokes second-order waves is obtained from the regular wave formulas in Section 2 by replacing U with U_c, i.e. the maximum near-bed orbital velocity under the wave crest, which will be elaborated further in

the forthcoming. The use of the regular wave formulas implies that each wave is treated individually, and consequently that the suspended sediment concentration is taken to be constant for a given wave situation and that memory effects are neglected. For rough turbulent flow the validity of this assumption was confirmed for seabed shear stresses by Holmedal et al. (2003) for high values of A/z_0 (at about 30000). Characteristic statistical values of the resulting seabed shear stress amplitude deviated less than 20% from those obtained by the Monte Carlo simulation method by Holmedal et al. (2000); that essentially is based on the same assumptions upon which the present approach is based. Regarding the assumption that each wave is treated individually, Holmedal et al. (2003) concluded for large values of A/z_0 that the main reason for the fair agreement obtained between the Monte Carlo simulations and the (k - ε) model predictions is the good description of the wave friction factor for individual waves. This appears to be much more important than violating the assumption of independent individual waves. Thus, since the suspended sediment concentration formulas applied here are essentially based on using the Shields parameter and the friction factor for rough turbulent flow in Eqs. (5) to (10), the assumption of treating each wave individually seems reasonable.

Moreover, the wave process is also assumed to be a stationary narrow-band process. For a narrow-band process the waves are specified as a 'harmonic' wave with cyclic frequency ω and with slowly varying amplitude and phase. Then, for the first order, the near-bed orbital velocity amplitude U is related to the near-bed orbital displacement amplitude A by $U = \omega A$, where U is slowly varying with time as well (see e.g. Sveshnikov (1966)). Thus this assumption is used as a first approximation to describe the stochastic features inherent in a random process, which consequently will provide results containing the global stochastic features associated with the random waves.

At a fixed point in a sea state with stationary narrow-band random waves consistent with Stokes second-order regular waves in finite water depth h the non-dimensional nonlinear

crest height, $w_c = \eta_c / a_{rms}$, and the non-dimensional nonlinear maximum horizontal particle velocity evaluated at the seabed, $\hat{U}_c = U_c / U_{rms}$, are (Dean and Dalrymple, 1984)

$$w_c = \hat{a} + O\left(k_p a_{rms}\right) \tag{25}$$

$$\hat{U}_c = \hat{a} + O\left(k_p a_{rms}\right) \tag{26}$$

Here $\hat{a} = a / a_{rms}$ is the non-dimensional linear wave amplitude, where the linear wave amplitude a is made dimensionless with the *rms* value a_{rms}, and

$$U_{rms} = \frac{\omega_p a_{rms}}{\sinh k_p h} \tag{27}$$

Moreover, $O\left(k_p a_{rms}\right)$ denotes the second order (nonlinear) terms which are proportional to the characteristic wave steepness of the sea state, $k_p a_{rms}$, where k_p is the wave number corresponding to ω_p (= the peak frequency of the wave spectrum) given by the dispersion relationship for linear waves (which is also valid for Stokes second order waves)

$$\omega_p^2 = g k_p \tanh k_p h \tag{28}$$

Now Eq. (25) can be inverted to give $\hat{a} = w_c - O\left(k_p a_{rms}\right)$, which substituted in Eq. (26) gives $\hat{U}_c = w_c + O\left(k_p a_{rms}\right)$. Thus it appears that $\hat{a}$ can be replaced with w_c in the linear term of $\hat{U}_c$, because the error involved is of second order. Consequently, by neglecting terms of $O\left(k_p a_{rms}\right)$ the maximum near-bed orbital velocity under the wave crest in dimensional form can be taken as

$$U_c = \frac{\omega_p \eta_c}{\sinh k_p h} \tag{29}$$

Moreover, $A_c = U_c / \omega_p$ is the maximum near-bed orbital displacement under the wave crest, $\hat{A}_c = A_c / A_{rms}$ is the non-dimensional maximum near-bed orbital displacement where

$$A_{rms} = \frac{a_{rms}}{\sinh k_p h} \tag{30}$$

Furthermore,

$$\omega_p = \frac{U_c}{A_c} = \frac{U_{rms}}{A_{rms}} \tag{31}$$

by combining Eqs. (27) and (30).

Now the Forristall (2000) parametric crest height distribution based on simulations using second-order theory is adopted. The simulations were based on the Sharma and Dean (1981) theory; this model includes both sum-frequency and difference-frequency effects. The simulations were made both for 2D and 3D random waves. A two-parameter Weibull distribution with the cumulative distribution function (*cdf*) of the form

$$P(w_c) = 1 - \exp\left[-\left(\frac{w_c}{\sqrt{8}\alpha}\right)^{\beta}\right] \; ; \; w_c \geq 0 \tag{32}$$

was fitted to the simulated wave data. The Weibull parameters α and β were estimated from the fit to the simulated wave data, and are based on the wave steepness S_1 and the Ursell parameter U_R defined by

$$S_1 = \frac{2\pi}{g}\frac{H_s}{T_1^2} \tag{33}$$

and

$$U_R = \frac{H_s}{k_1^2 h^3} \tag{34}$$

Here H_s is the significant wave height, T_1 is the spectral mean wave period, and k_1 is the wave number corresponding to T_1. It should be noted that $H_s = 2\sqrt{2}a_{rms}$ when a is Rayleigh distributed. The wave steepness and the Ursell number characterize the degree of nonlinearity of the waves in finite water depth. At zero steepness and zero Ursell number the fits were

forced to match the Rayleigh distribution, i.e. $\alpha = 1/\sqrt{8} \approx 0.3536$ and $\beta = 2$. Note that this is the case for both 2D and 3D linear waves. The resulting parameters for the 2D-model are

$$\begin{aligned} \alpha_{2D} &= 0.3536 + 0.2892 S_1 + 0.1060 U_R \\ \beta_{2D} &= 2 - 2.1597 S_1 + 0.0968 U_R^2 \end{aligned} \tag{35}$$

and for the 3D-model

$$\begin{aligned} \alpha_{3D} &= 0.3536 + 0.2568 S_1 + 0.0800 U_R \\ \beta_{3D} &= 2 - 1.7912 S_1 - 0.5302 U_R + 0.284 U_R^2 \end{aligned} \tag{36}$$

Forristall (2000) demonstrated that the wave setdown effects were smaller for short-crested than for long-crested waves, which is due to that the second-order negative difference-frequency terms are smaller for 3D waves than for 2D waves. Consequently the wave crest heights are larger for 3D waves than for 2D waves.

3.2 Outline of stochastic method

Let x represent the random variable which causes the sand grains to be suspended, i.e. the crest velocity due to second-order waves. The quantity of interest is the expected (mean) suspended sediment concentration caused by the random waves

$$E[\mathrm{C(z)}] = \int_0^\infty C(z;x)p(x)dx \tag{37}$$

where $p(x)$ is the probability density function (*pdf*) of x. More specifically, the present approach is based on the following assumptions: the free surface elevation is a stationary narrow-band process with zero expectation, and that the formulas for regular waves given in Section 2 are valid for individual irregular waves as well.

3.3 Rippled beds

For a narrow-band process $T = T_p$ where $T_p = 2\pi / \omega_p = 2\pi A_{rms} / U_{rms}$ and where Eq. (31) has been used. By taking $U = U_c$, $A = A_c$ and using from Eq. (31) that $\hat{A} \equiv A_c / A_{rms} = U_c / U_{rms} \equiv \hat{U}_c$, Eqs. (1) to (15) can be combined and re-arranged to be valid for individual random waves. This means that Eq. (1) is valid together with the following equations (with $\hat{U}_c = w_c$ by neglecting terms of $O(k_p a_{rms})$ according to the previous discussion) :

$$\ell = 0.075 \frac{U_{rms} \eta}{w_s} w_c \quad \text{for} \quad \frac{U_{rms}}{w_s} < 18 \tag{38}$$

$$\ell = 1.4\eta \quad \text{for} \quad \frac{U_{rms}}{w_s} \geq 18 \tag{39}$$

$$C_0 = 0.005\theta_r^3 \; ; \; \theta_r = \frac{\theta_{rms} w_c^{2-d}}{\left(1 - \pi \dfrac{\eta}{\lambda}\right)^2} \tag{40}$$

$$\theta = \theta_{rms} w_c^{2-d} \; ; \; \theta_{rms} = \frac{\dfrac{1}{2} c \left(\dfrac{A_{rms}}{z_0}\right)^{-d} U_{rms}^2}{g(s-1) d_{50}} \tag{41}$$

$$\eta = 21 \psi_{rms}^{-1.85} A_{rms} w_c^{-2.70} \quad \text{for} \quad \psi_{rms} > 10 \tag{42}$$

$$\frac{\eta}{\lambda} = 0.342 - 0.340 \theta_{rms}^{0.25} w_c^{(2-d)/4} \tag{43}$$

$$\psi_{rms} = \frac{U_{rms}^2}{g(s-1) d_{50}} \tag{44}$$

Now the mean suspended sediment concentration at an elevation z above the seabed caused by the random waves is given from Eq. (37) as

$$E[C(z)] = \int_0^\infty C(z; w_c) p(w_c) dw_c \tag{45}$$

where $C(z; w_c)$ is given by Eqs. (1), (11), (12) and (38) to (44), and $p(w_c)$ is obtained from

the *cdf* of w_c in Eq. (32). However, since Eq. (14) is valid for $\theta < 0.8$ it implies that $\hat{U}_c = w_c$ follows the truncated Weibull distribution given by the *cdf*

$$P(w_c) = \frac{1-\exp\left[-\left(\frac{w_c}{\sqrt{8}\alpha}\right)^{\beta}\right]}{1-\exp\left[-\left(\frac{w_{c2}}{\sqrt{8}\alpha}\right)^{\beta}\right]}; 0 \le w_c \le w_{c2} \tag{46}$$

where $w_{c2} = (\theta_c / \theta_{rms})^{1/(2-d)}$ and $\theta_c = 0.8$ and by using Eq. (41).

It should also be noted that when evaluating the integral in Eq. (45) it is checked that the Shields criterion $\theta = \theta_{rms} w_c^{2-d} > \theta_{cr}$ is valid for each individual wave.

3.4 Sheet flow

Similar to the procedure in Section 3.3, Eqs. (17) to (19), (23) and (24) can be combined and re-arranged to be valid for individual random waves. This means that Eq. (17) is valid together with the following equations:

$$C_a = \frac{0.331\left[\theta_{rms} w_c^{2-d}\left(1+\frac{\delta_{rms}}{\omega_p} w_c\right)-0.045\right]^{1.75}}{1+0.720\left[\theta_{rms} w_c^{2-d}\left(1+\frac{\delta_{rms}}{\omega_p} w_c\right)-0.045\right]^{1.75}} \tag{47}$$

$$u_* = \left[g(s-1)d_{50}\theta_{rms}\right]^{1/2}\left[w_c^{2-d}\left(1+\frac{\delta_{rms}}{\omega_p} w_c\right)\right]^{1/2} \tag{48}$$

$$\delta_{rms} = \frac{1}{2\sqrt{2}} k_p A_{rms} \tag{49}$$

Now the mean suspended sediment concentration at an elevation z above the seabed caused by the random waves is given from Eq. (37) as

$$E[C(z)] = \int_0^{\infty} C(z; w_c) p(w_c) dw_c \tag{50}$$

where $C(z;w_c)$ is given by Eqs. (17), (47) to (50), and $p(w_c)$ is obtained from the *cdf* of w_c in Eq. (31). However, since Eq. (14) is valid for $\theta > 0.8$ it implies that $\hat{U}_c = w_c$ is defined in a finite interval. Consequently w_c follows the truncated Weibull distribution given by the *cdf*

$$P(w_c) = \frac{\exp\left[-(\frac{w_{c1}}{\sqrt{8}\alpha})^{\beta}\right] - \exp\left[-(\frac{w_c}{\sqrt{8}\alpha})^{\beta}\right]}{\exp\left[-(\frac{w_{c1}}{\sqrt{8}\alpha})^{\beta}\right]}; w_{c1} \le w_c \tag{51}$$

where $w_{c1} = (\theta_c / \theta_{rms})^{1/(2-d)}$ and $\theta_c = 0.8$ and by using Eq. (51). The integral on the right-hand side of Eq. (50) has to be calculated numerically.

Formally this formulation includes both second-order wave asymmetry and wave boundary layer streaming effects. However, based on the background given in the Introduction, it should be noted that the method is only valid for each of the effects separately. More specifically this means that:

1. The effect of second-order wave asymmetry is taken into account by taking $\delta_{rms} = 0$ in Eqs. (47) and (48) and by using the *cdf* in Eq. (51) with S_1 and U_R over their whole validity range.
2. The effects of wave boundary layer streaming is taken into account by taking $\delta_{rms} \neq 0$ and by using the *cdf* in Eq. (51) with $S_1 = 0$ and $U_R = 0$, i.e. the Rayleigh *cdf* mode of Eq. (51) corresponding to linear waves.

4. RESULTS AND DISCUSSION

Now some results for the mean suspended sediment concentration over rippled beds and for sheet flow will be presented and discussed. First, predictions by the present approach will be compared with results from the Thorne et al.'s (2002) experimental study for random wave-induced flow over rippled bedforms. Second, since to the authors' knowledge no data exist in

the open literature on suspended concentration for random wave-induced sheet flow, an example of results is provided for sheet flow conditions.

4.1 Comparisons with Thorne et al.'s (2002) data for rippled beds

Predictions by the present approach will now be compared with results from the experimental study reported by Thorne et al. (2002). They presented results on data obtained from measurements of suspended sediment concentrations over rippled bedforms beneath both 2D regular and random waves in a large-scale flume. Here the random wave data from four experiments are considered. The sediment consists of medium quartz sand with $d_{10} = 0.175\,\text{mm}$, $d_{50} = 0.33\,\text{mm}$ and $d_{90} = 0.735\,\text{mm}$, which is the grain diameter corresponding to 10, 50 and 90 percent of the material being finer than the given value, respectively. The other main flow variables are given in Table 1.

The present stochastic approach requires knowledge of T_z, A_{rms} and U_{rms}. Since the wave process is assumed to be narrow-banded it follows that $T_z = T_p$. Consequently $U_{rms} = \omega_p A_{rms}$, $A_{rms} = H_{rms} / \left(2\sinh \bar{k}h\right) = H_{rms} / \left(2\sinh k_p h\right)$ where $H_{rms} = H_s / \sqrt{2}$ when H is Rayleigh distributed, and $\bar{k}$ and k_p are the wave numbers corresponding to the wave frequencies $\omega_z \left(\omega_z^2 = g\bar{k}\tanh \bar{k}h\right)$ and $\omega_p \left(\omega_p^2 = gk_p \tanh k_p h\right)$, respectively. Thus the procedure is to determine k_p for given values of ω_p and h from $\omega_p^2 = gk_p \tanh k_p h$, and to calculate A_{rms} and U_{rms}.

The predictions are based on two modes of the method:

- The full stochastic method as described in Section 3.3.
- The semi-stochastic method; similar to the full stochastic method except for specifying the ripple geometry; i.e. not applying Eqs. (42) and (43), but otherwise the method is as described in Section 3.3.

Figs. 1 to 4 show the mean concentration versus the height z above the seabed for Experiments 11 (Fig. 1), 12 (Fig. 2), 13 (Fig. 3) and 14 (Fig. 4). The data are represented by the mean value (dots) and the mean value ±25% (crosses). The four curves in each figure represent the predictions; the full stochastic method for linear and 2D nonlinear waves; the semi-stochastic method for linear and 2D nonlinear waves. It should be noted that in the semi-stochastic method the ripple geometry (i.e. η and λ) given in Table 1 is used as input for both linear and 2D nonlinear waves. Moreover, the scales along the horizontal axis are different in the figures, reflecting that the suspended concentration increases as H_s increases from Figs. 1 to 4 (see also Table 1).

Overall, from the results shown in Figs. 1 to 4 it appears that the semi-stochastic method is superior to the full stochastic method. The main reason is most probably that by using the measured ripple geometry the uncertainties of determining the reference concentration is reduced compared with using the full stochastic method.

It should be noted that Thorne et al. (2002) compared predictions with the measured suspended sediment concentration for Experiment 14. Essentially the predictions were made by using a deterministic method and with the measured bedform as input. More specifically, they considered the concentration profile obtained by pure diffusion (i.e. corresponding to Eq. (1)), pure convection and combined convection–diffusion following the formulations in Nielsen (1992). They obtained good prediction of the data in Experiment 14 by making a best fit to the data by the combined convection-diffusion solution.

4.2 Example of results for sheet flow

An example for sheet flow based on the results in Section 3.4 is presented by using the following given flow conditions: $h=15\,\text{m}$, $H_s=5\,\text{m}$, $T_p=8.9\,\text{s}$, $d_{50}=0.20\,\text{mm}$, $s=2.65$, $w_s=0.02\,\text{m/s}$ (Eq. (11)). The calculated quantities are given Table 2. It appears that the flow

corresponds to sheet flow conditions, i.e. $\theta_{rms} = 1.124 > 0.8$. Fig. 5 shows the mean suspended concentration versus the height above the bed for these flow conditions. The results are given for linear waves, 2D and 3D nonlinear waves (i.e. no streaming included), streaming and linear waves including streaming. It appears that the mean concentration is: slightly larger for 3D than for 2D nonlinear waves, which both are larger than that for linear waves as well as for linear waves including streaming. These features are also demonstrated in Fig. 6, showing the following ratios: the nonlinear to linear ratios for 2D ($R_{1,2D}$) and 3D ($R_{1,3D}$) waves; the ratio between the mean concentration for 3D waves and the mean concentration for 2D waves (R_2); the ratio between the mean concentration due to streaming and that for linear waves (R_{str}); the ratio between the mean concentration due to streaming and that for 2D nonlinear waves (R_3). From Fig. 6 it appears that $R_{1,2D}$ and $R_{1,3D}$ range up to about 1.7 and 1.9, respectively. Consequently, R_2 ranges up to about 1.1. Moreover, R_{str} and R_3 range up to about 0.3 and 0.1, respectively. The larger concentration for 3D waves than for 2D waves is caused by the smaller wave setdown effect for short-crested than for long-crested waves as mentioned previously in Section 3.1. This smaller wave setdown effect for 3D than for 2D waves leads to higher wave crests and therefore larger wave-induced bed shear stress under the wave crest for 3D waves than for 2D waves. Consequently this gives larger concentration for 3D waves than for 2D waves.

4.3 General comments

It should be noted that the effects of wave nonlinearity due to 2D and 3D Stokes second order waves are not possible to estimate by using the deterministic method since nonlinearities are not included in the regular wave formulas. Hence this stochastic approach is more mathematically sound than by using H_{rms} and T_p in an otherwise deterministic method.

Moreover, it also provides results which arise from 2D and 3D Stokes second order wave nonlinearities inherent in the Forristall (2000) parametric wave crest distribution. However, comparison with more data is required to validate the approach. In the meantime the approach should be of practical interest for estimating random wave-induced suspended sediment concentrations based on available wave statistics.

5. CONCLUSIONS

The main conclusions are:

1. A practical stochastic method for calculating the suspended sediment concentration due to random waves is given for:
   - A rippled seabed including effects of second order wave asymmetry;
   - Sheet flow including separate effects of second order wave asymmetry and boundary layer streaming.
2. The method includes two modes:
   - Full stochastic method for rippled beds and sheet flow;
   - Semi-stochastic method for rippled beds, i.e. by specifying the ripple geometry, but otherwise a stochastic method.
3. Overall, for rippled beds the semi-stochastic method gives better prediction of the Thorne et al. (2002) data than the full stochastic method. The main reason is most probably that by using the measured ripple geometry as input the uncertainties of determining the reference concentration is reduced compared with using the full stochastic method.
4. For sheet flow an example of results shows that

$$C(z)_{3Dnonlinear} > C(z)_{2Dnonlinear} > C(z)_{linear+streaming} > C(z)_{linear}$$

The larger $C(z)$ for 3D than for 2D nonlinear waves is attributed to the smaller wave

setdown effects for 3D waves than for 2D waves.

5. The present results for sheet flow should be taken as tentative, and data for comparison are required before any conclusion can be made regarding the validity of the approach. In the meantime, the method should be useful as an engineering tool for the assessment of streaming effects on suspended sediments due to random waves.

ACKNOWLEDGEMENT

This work was carried out as part of the project "Air-Sea Interaction and Transport Mechanisms in the Ocean" funded by the Norwegian Research Council. This support is gratefully acknowledged.

REFERENCES

Bolanos, R., Thorne, P.D., Wolf, J. (2012). Comparison of measurements and models of bed stress, bedforms and suspended sediments under combined currents and waves. *Coastal Eng.*, 62, 19-30.

Cacchione, D.A., Thorne, P.D., Agrawal, Y., Nidzieko, N.J. (2008). Time-averaged near-bed suspended sediment concentrations under waves and currents: Comparison of measured and model estimates. *Continental Shelf Res.*, 28, 470-484.

Chassagneux, F.X., Hurther, D. (2014). Wave bottom boundary layer processes below irregular surfzone breaking waves with light-weight sheet flow particle transport. *J. Geophys. Res.*,119, 1668-1690, doi:10.1002/2013JC009338.

Davies, A.G., Villaret, C. (1997). Oscillatory flow over rippled beds: Boundary layer structure and wave-induced Eulerian drift. In: Hunt, J.N., editor. Gravity Waves in Water of Finite Depth. *Advances in Fluid Mechanics*, pp. 215-254, Chapter 6.

Davies, A.G., Villaret, C. (1998). Wave-induced currents above rippled beds. In: Dronkers, J., Scheffers, M., editors. *Physics of Estuaries and Coastal Seas.* Rotterdam: A.A. Balkema.

Davies, A.G., Villaret, C. (1999). Eulerian drift induced by progressive waves above rippled and very rough beds. *J. Geophys. Res.* 104(C1): 1465-1488.

Dean, R.G., Dalrymple, R.A. (1984). *Water Wave Mechanics for Engineers and Scientists.* Prentice Hall, Inc., New Jersey, USA.

Dolphin, T., Vincent, C. (2009). The influence of bed forms on reference concentration and suspension under waves and currents. *Continental Shelf Res.*, 29, 424-432.

Forristall, G.Z. (2000). Wave crest distributions: Observations and second-order theory. *J. Phys. Oceanography*, 30, 1931-1943.

Fuhrman, D.R., Schløer, S., Sterner, S. (2013). RANS-based simulation of turbulent wave boundary layer and sheet flow sediment transport processes. *Coastal Eng.*, 73,151-166.

Holmedal, L.E., Johari, J., Myrhaug, D. (2013). The seabed boundary layer beneath waves opposing and following a current. *Continental Shelf Res.*, 65, 27-44.

Holmedal, L.E., Myrhaug, D. (2009). Wave-induced steady streaming, mass transport and net sediment transport in rough turbulent ocean bottom boundary layers. *Continental Shelf Res.*, 29, 911-926.

Holmedal, L.E., Myrhaug, D., Rue, H. (2000). Seabed shear stresses under irregular waves plus current from Monte Carlo simulations of parameterized models. *Coastal Eng.*, 39, 123-147.

Holmedal, L.E., Myrhaug, D., Rue, H. (2003). The seabed boundary layer under random waves plus current. *Cont. Shelf Res.*, 23 (7), 717-750, erratum 1035.

Longuet-Higgins, M.S. (1956). The mechanics of the boundary layer near the bottom

in a progressive wave. *Proc.6th Int. Conf. Coastal Eng., ASCE,* Miami 1956; 184-193.

Myrhaug, D., Holmedal, L.E. (2007). Mobile layer thickness in sheet flow beneath random waves. *Coastal Eng.*, 54, 577-585.

Myrhaug, D., Holmedal, L.E., Rue, H. (2004). Bottom friction and bedload sediment transport caused by boundary layer streaming beneath random waves. *Applied Ocean Res.*, 26, 183-197.

Myrhaug, D., Holmedal, L.E., Simons, R.R., MacIver, R.D. (2001). Bottom friction in random waves plus current flow. *Coastal Eng.*, 43, 75-92.

Nielsen, P. (1992). *Coastal Bottom Boundary Layers and Sediment Transport.* World Scientific Publishing, Singapore.

Nielsen, P., Callaghan, D.P. (2003). Shear stress and sediment transport calculations for sheet flow under waves. *Coastal Eng.*, 47, 347-354.

Sharma, J.N., Dean, R.G. (1981). Second-order directional seas and associated wave forces. *Soc. of Petroleum Engineers Journal,* 21, 129-140.

Soulsby, R.L. (1997). *Dynamics of Marine Sands*. Thomas Telford, London.

Sveshnikov, A.A. (1966). *Applied Methods in the Theory of Random Functions.* Pergamon Press, New York.

Thorne, P.D., Williams, J.J., Davies, A.G. (2002). Suspended sediments under waves measured in a large-scale flume facility. *J. Geophys. Res.*, 107 (C8), 3178.

Trowbridge, J., Madsen, O.S. (1984). Turbulent wave boundary layers. Second-order theory and mass transport. *J. Geophys Res.* 89(CS), 7999-8007.

Zyserman, J.A., Fredsøe, J. (1994). Data analysis of bed concentration of suspended sediment. *J. of Hydraulic Res.*, 120 (9), 1021-1042.

Table 1. The main flow variables in Thorne et al.'s (2002) measurements.

Experiment	h (m)	H_s (m)	T_p (s)	η (m)	λ (m)
11	4.46	0.504	4.98	0.040	0.262
12	4.5	0.788	4.92	0.045	0.325
13	4.5	1.006	5.10	0.046	0.395
14	4.5	1.223	5.10	0.056	0.480

Table 2. The main flow variables in the example of results for sheet flow.

$H_{rms}(m)$	3.54
k_p (rad/m)	0.0667
S_1	0.040
U_R	0.333
U_{rms}(m/s)	1.06
A_{rms} (m)	1.50
A_{rms} / z_0	90 000
c, d	0.112, 0.25
θ_{rms} (Eq. (41))	1.14
δ_{rms} (Eq. (47))	0.0354

Figure captions

Fig 1 Experiment 11: measured and predicted concentration profiles above a rippled bed; the data are from Thorne et al. (2002); see also Table 1.

Fig. 2 Experiment 12: otherwise caption as in Fig. 1.

Fig. 3 Experiments 13: otherwise caption as in Fig. 1.

Fig. 4 Experiment 14: otherwise caption as in Fig. 1.

Fig. 5 Example of results for sheet flow: mean concentration profile above the bed for h=15m, H_s=5 m, T_p=8.9 s, d_{50}=0.20 mm, s=2.65, w_s = 0.02 m/s; see also Table 2.

Fig. 6 Ratios for the mean concentration profiles above the bed for the example of results presented in Fig. 5.

Figure

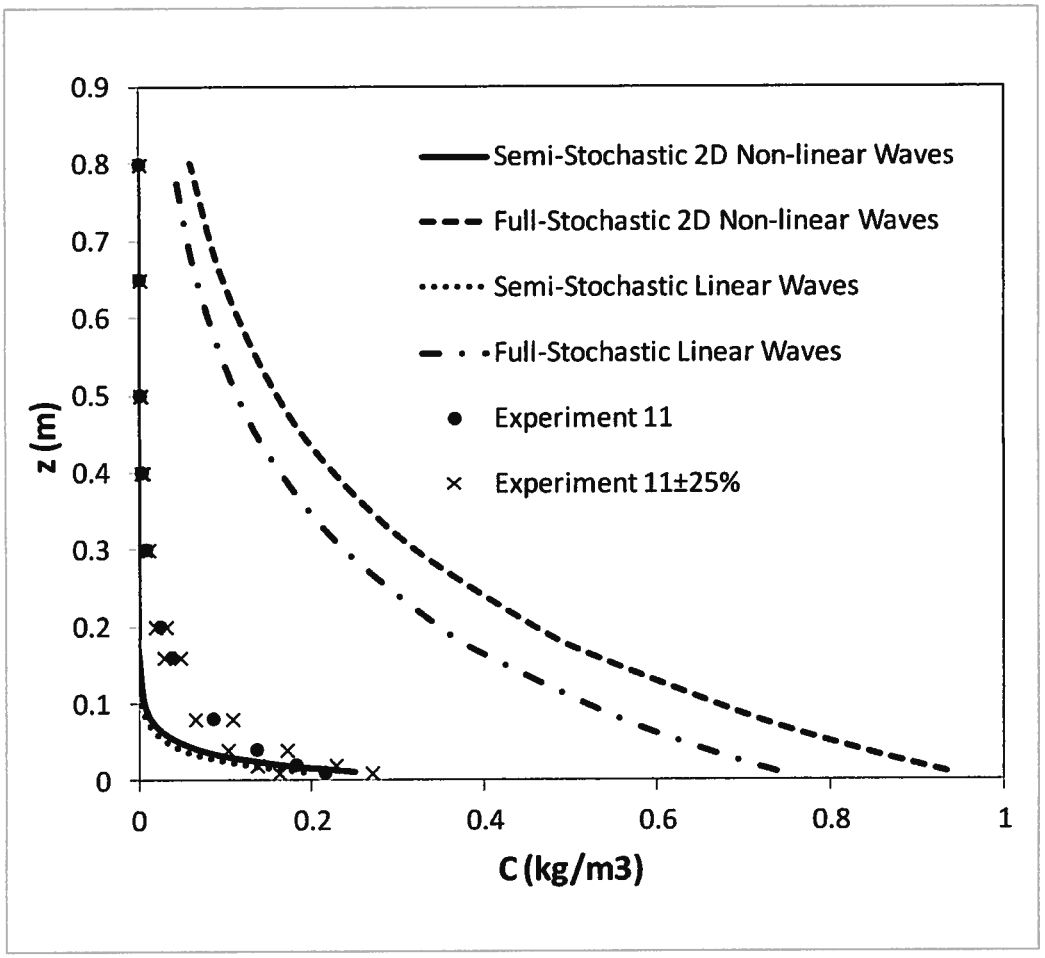

Fig 1 Experiment 11: measured and predicted concentration profiles above a rippled bed; the data are from Thorne et al. (2002); see also Table 1.

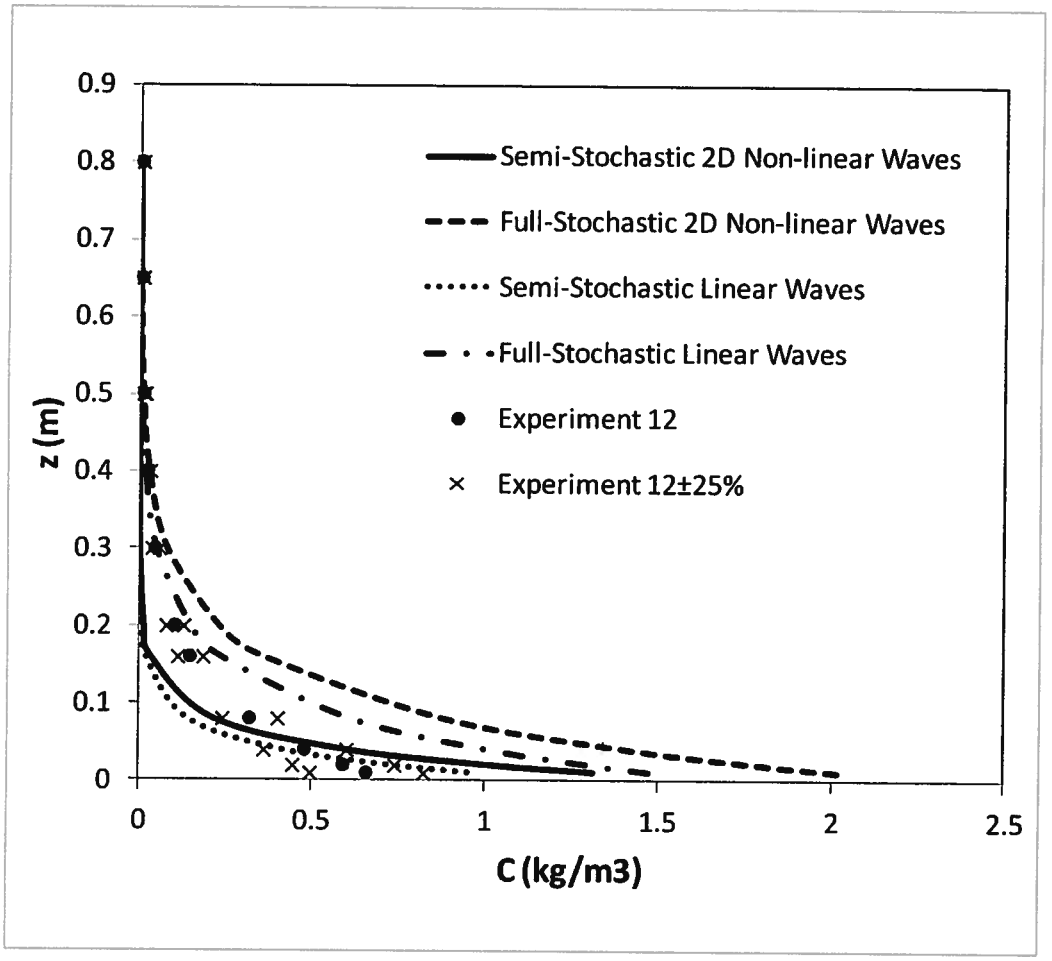

Fig. 2 Experiment 12: otherwise caption as in Fig. 1.

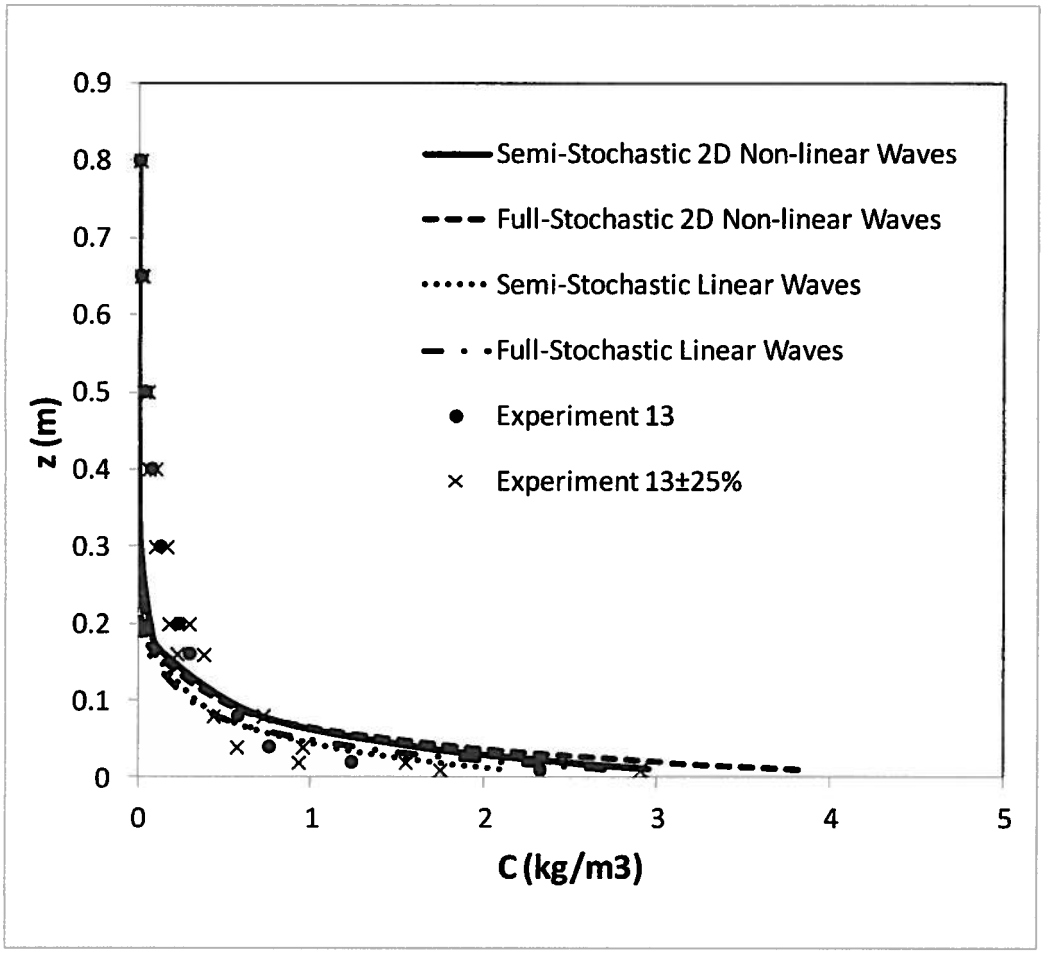

Fig. 3 Experiment 13: otherwise caption as in Fig. 1.

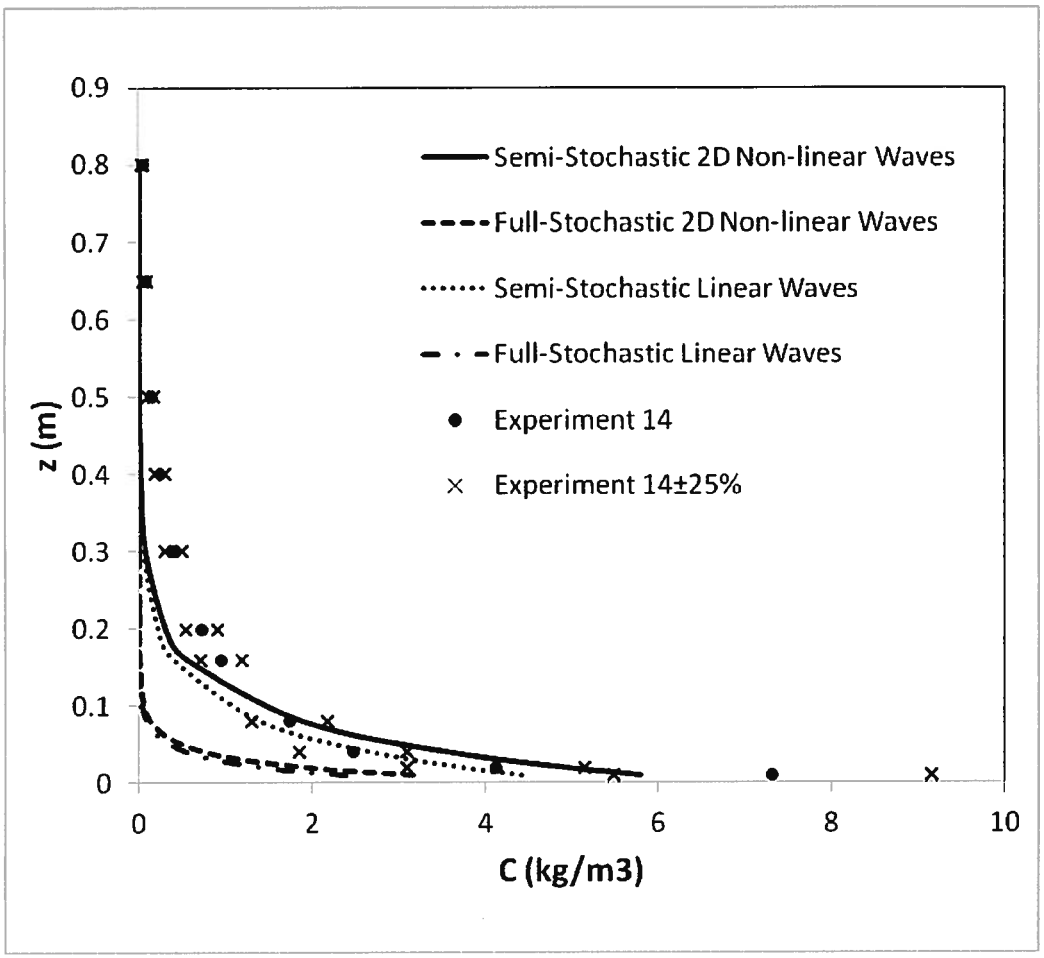

Fig. 4 Experiment 14: otherwise caption as in Fig. 1.

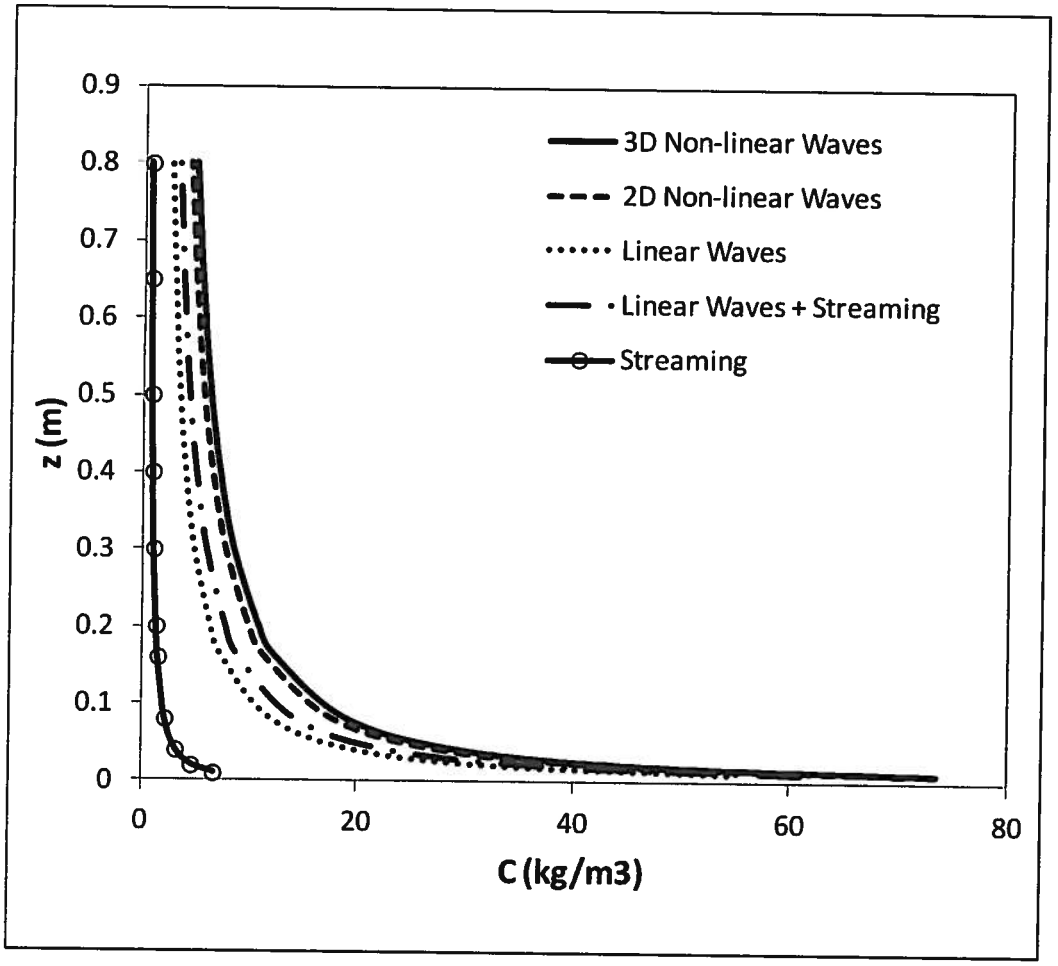

Fig. 5 Example of results for sheet flow: mean concentration profile above the bed for h=15m, H_s=5 m, T_p=8.9 s, d_{50}=0.20 mm, s=2.65, w_s = 0.02 m/s; see also Table 2.

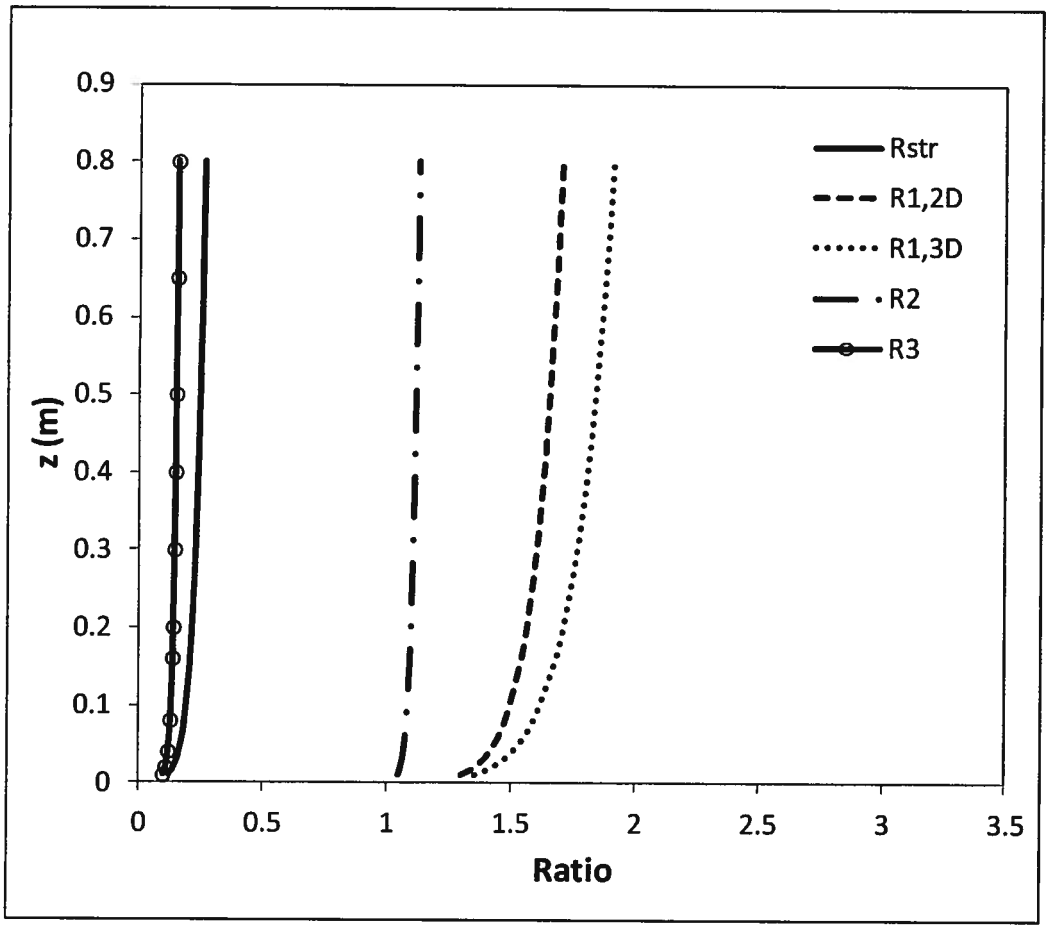

Fig. 6 Ratios for the mean concentration profiles above the bed for the example of results presented in Fig. 5.